THE UNIVERSITY OF
WARWICK

Author(s): J. Southworth, C. M. Copperwheat, B. T. Gänsicke and S. Pyrzas
Article Title: Orbital periods of cataclysmic variables identified by the SDSS - VII. Four new eclipsing systems
Year of publication: 2010
Link to published article:
http://dx.doi.org/10.1051/0004-6361/200913576
Publisher statement: © ESO 2010. J. Southworth et al. (2010). Orbital periods of cataclysmic variables identified by the SDSS - VII. Four new eclipsing systems. Astronomy & Astrophysics, Vol.510.

Astronomy & Astrophysics

Orbital periods of cataclysmic variables identified by the SDSS

VII. Four new eclipsing systems[⋆]

J. Southworth[1,2], C. M. Copperwheat[2], B. T. Gänsicke[2], and S. Pyrzas[2,3]

[1] Astrophysics Group, Keele University, Newcastle-under-Lyme, ST5 5BG, UK
   e-mail: jkt@astro.keele.ac.uk
[2] Department of Physics, University of Warwick, Coventry, CV4 7AL, UK
[3] Isaac Newton Group of Telescopes, Apartado de Correos 321, 38700 Santa Cruz de La Palma, Spain

ABSTRACT

We present photometry of nine cataclysmic variable stars identified by the Sloan Digital Sky Survey, aimed at measuring the orbital periods of these systems. Four of these objects show deep eclipses, from which we measure their orbital periods. The light curves of three of the eclipsing systems are also analysed using the LCURVE code, and their mass ratios and orbital inclinations determined. SDSS J075059.97+141150.1 has an orbital period of 134.1564 ± 0.0008 min, making it a useful object with which to investigate the evolutionary processes of cataclysmic variables. SDSS J092444.48+080150.9 has a period of 131.2432 ± 0.0014 min and is probably magnetic. The white dwarf ingress and egress phases are very deep and short, and there is no clear evidence that this object has an accretion disc. SDSS J115207.00+404947.8 and SDSS J152419.33+220920.1 are nearly identical twins, with periods of 97.5 ± 0.4 and 93.6 ± 0.5 min and mass ratios of 0.14 ± 0.03 and 0.17 ± 0.03, respectively. Their eclipses have well-defined white dwarf and bright spot ingress and egress features, making them excellent candidates for detailed study. All four of the orbital periods presented here are shorter than the 2–3 h period gap observed in the known population of cataclysmic variables.

Key words. dwarf novae – novae, cataclysmic variables – binaries: eclipsing – binaries: spectroscopic – white dwarfs

1. Introduction

Cataclysmic variables (CVs) are interacting binary stars containing a white dwarf primary component in a close orbit with a low-mass secondary star which fills its Roche lobe. In most of these systems the secondary component is hydrogen-rich and transfers material to the white dwarf via an accretion disc. Comprehensive reviews of the properties of CVs have been given by Warner (1995) and Hellier (2001). CVs are thought to evolve from longer to shorter orbital periods through the loss of orbital angular momentum, before reaching a minimum period caused by the changes in the structure of the mass donor and evolving back to longer periods. However, theoretical population synthesis models of this scenario (de Kool 1992; de Kool & Ritter 1993; Kolb 1993; Kolb & de Kool 1993; Politano 1996, 2004; Kolb & Baraffe 1999) are unable to reproduce the orbital period distribution of the observed population of CVs (Downes et al. 2001; Ritter & Kolb 2003).

This disagreement may mainly be due to observational selection effects favouring the discovery and analysis of longer-period CVs, which are intrinsically much brighter than their shorter-period colleagues. We are therefore working on the characterisation of the population of CVs discovered by the Sloan Digital Sky Survey (SDSS[1]; see Szkody et al. 2007, and references therein), which were identified spectroscopically so should be much less affected by these selection biases. Further information and previous results can be found in Gänsicke et al. (2006), Southworth et al. (2006, 2007a,b, 2008a,b) and Dillon et al. (2008). A major recent result of our project is the identification of the long-predicted pile-up of objects at the minimum period (the "period spike"), which is discussed in detail by Gänsicke et al. (2009).

In this work we present and analyse time-resolved photometry of four CVs which we have discovered to show eclipses. We abbreviate the names of the targets to SDSS J*nnnn*, where *nnnn* are the first four digits of right ascension. The full and abbreviated names, references and *ugriz* apparent magnitudes are given in Table 1. In Fig. 1 we plot their SDSS spectra for reference. In Sect. 8 we also present light curves of five SDSS CVs for which we did not find periodic brightness variations.

2. Observations and data reduction

Most of the observations presented in this work were obtained in 2009 January using the New Technology Telescope (NTT) at ESO La Silla, equipped with the EFOSC2 focal-reducing instrument[2] (Buzzoni et al. 1984). We used EFOSC2 in imaging mode and with a Loral 2048×2048 px² CCD binned 2×2, giving a field of view of 4.4×4.4 arcmin² at a plate scale of $0.26''$ px⁻¹. All images were obtained with a B_{Tyson} filter (ESO filter #724), which has a central wavelength of 4445 Å and a *FWHM* of 1838 Å.

---

[1] http://www.sdss.org/

[2] http://www.eso.org/sci/facilities/lasilla/instruments/efosc/index.html

Table 1. Full names, references and SDSS *ugriz* apparent magnitudes of our targets.

SDSS name	Short name	Reference	u	g	r	i	z	$g_{\rm spec}$
SDSS J031051.66−075500.2	SDSS J0310	Szkody et al. (2003)	15.76	15.49	15.74	15.89	16.10	22.03
SDSS J074355.55+183834.8	SDSS J0743	Szkody et al. (2006)	20.11	20.07	19.29	18.78	18.61	21.66
SDSS J074640.61+173412.7	SDSS J0746	Szkody et al. (2006)	18.21	18.16	18.37	18.52	18.55	21.20
SDSS J075059.97+141150.1	SDSS J0750	Szkody et al. (2007)	19.20	19.09	18.98	18.79	18.58	18.83
SDSS J075808.81+104345.5	SDSS J0758	Szkody et al. (2009)	17.06	16.92	17.07	17.17	17.25	17.06
SDSS J090628.24+052656.9	SDSS J0906	Szkody et al. (2005)	18.82	18.76	18.46	18.10	17.82	19.32
SDSS J092444.48+080150.9	SDSS J0924	Szkody et al. (2005)	19.49	19.25	19.26	18.70	17.88	19.36
SDSS J115207.00+404947.8	SDSS J1152	Szkody et al. (2007)	19.22	19.26	19.15	19.13	19.00	19.56
SDSS J152419.33+220920.1	SDSS J1524	Szkody et al. (2009)	19.04	19.04	18.90	18.80	18.50	19.52

Notes. $g_{\rm spec}$ is an apparent magnitude calculated by convolving the SDSS flux-calibrated spectra with the g passband function. These represent a different epoch to the SDSS *ugriz* magnitudes, but may be affected by "slit losses" due to any errors in astrometry or positioning of the fibre entrance.

Table 2. Log of the observations presented in this work.

Target	Date (UT)	Start time (UT)	End time (UT)	Telescope and instrument	Optical element	Number of observations	Exposure time (s)	Mean magnitude
SDSS J0310	2009 01 25	00:56	03:40	NTT/EFOSC2	$B_{\rm Tyson}$ filter	105	60	21.3
SDSS J0743	2009 01 23	01:36	03:37	NTT/EFOSC2	$B_{\rm Tyson}$ filter	80	40–60	22.3
SDSS J0743	2009 01 23	05:39	06:43	NTT/EFOSC2	$B_{\rm Tyson}$ filter	42	60	22.2
SDSS J0746	2009 01 24	01:01	03:44	NTT/EFOSC2	$B_{\rm Tyson}$ filter	123	30–60	20.2
SDSS J0746	2009 01 24	06:09	07:12	NTT/EFOSC2	$B_{\rm Tyson}$ filter	59	30	20.4
SDSS J0750	2009 01 22	00:53	05:27	NTT/EFOSC2	$B_{\rm Tyson}$ filter	255	30	19.2
SDSS J0750	2009 01 23	01:07	01:30	NTT/EFOSC2	$B_{\rm Tyson}$ filter	22	30	19.3
SDSS J0750	2009 01 26	02:50	03:33	NTT/EFOSC2	$B_{\rm Tyson}$ filter	41	30	19.4
SDSS J0750	2009 01 27	00:57	01:37	NTT/EFOSC2	$B_{\rm Tyson}$ filter	34	40	19.5
SDSS J0750	2009 02 16	22:04	22:31	WHT/Aux	V filter	164	5	18.9
SDSS J0758	2009 01 26	00:55	02:46	NTT/EFOSC2	$B_{\rm Tyson}$ filter	150	10	17.3
SDSS J0758	2009 01 26	04:37	04:57	NTT/EFOSC2	$B_{\rm Tyson}$ filter	28	10	17.3
SDSS J0906	2008 01 18	04:07	06:12	INT/WFC	g filter	69	70	18.9
SDSS J0906	2008 01 20	03:15	06:01	INT/WFC	g filter	112	60	18.4
SDSS J0906	2009 01 24	03:49	06:04	NTT/EFOSC2	$B_{\rm Tyson}$ filter	125	30	19.4
SDSS J0906	2009 01 24	07:16	09:17	NTT/EFOSC2	$B_{\rm Tyson}$ filter	113	30	19.4
SDSS J0906	2009 01 27	01:43	03:28	NTT/EFOSC2	R filter	85	40	19.4
SDSS J0924	2009 01 25	03:46	07:29	NTT/EFOSC2	$B_{\rm Tyson}$ filter	207	30	21.1
SDSS J0924	2009 01 26	05:00	05:21	NTT/EFOSC2	$B_{\rm Tyson}$ filter	20	30	21.4
SDSS J0924	2009 01 27	05:04	05:34	NTT/EFOSC2	$B_{\rm Tyson}$ filter	29	30	21.3
SDSS J0924	2009 02 16	23:51	00:10	WHT/Aux	V filter	75	10	18.9
SDSS J1152	2009 02 17	00:16	02:36	WHT/Aux	V filter	564	10	19.6
SDSS J1524	2009 05 06	02:58	05:43	WHT/Aux	V filter	756	10	19.1

Notes. The mean magnitudes are formed from observations outside eclipses only.

Additional observations were obtained in 2009 February (classical observing) and May (service mode) at the William Herschel Telescope (WHT) at La Palma. For these we used the Auxiliary Port focal station, which was equipped at the time with the EEV 4200×2048 px^2 CCD destined for the ACAM instrument[3]. The CCD was binned 4×4 and windowed down to the central 2048×2100 pixels, which reduced the dead time between exposures to only 5 s whilst still properly sampling the seeing conditions (plate scale 0.27″ px^{-1}) and available field of view (a circle of 1.8 arcmin in diameter). We used the Johnson V filter for all WHT observations.

The data were reduced using standard methods, with a pipeline written in IDL[4] (Southworth et al. 2009b,c,d). Aperture photometry was performed using the ASTROLIB/APER procedure[5], which originates from DAOPHOT (Stetson 1987). For the NTT we were able to set the photometry apertures by eye and fix their positions, whereas for the WHT they were set by eye and adjusted according to the offset between each image and the reference image found by cross-correlation.

Light curves of SDSS J0906 were obtained on the nights of 2008/01/17 and 2008/01/19 using the Isaac Newton Telescope (INT) and Wide Field Camera (WFC) equipped with a g filter. These data were reduced using the pipeline described by Gänsicke et al. (2004), which performs aperture photometry via the SExtractor package (Bertin & Arnouts 1996).

The instrumental differential magnitudes have been transformed to BV apparent magnitudes using formulae from Jordi et al. (2006). Given the non-standard nature of the spectral

---

[3] http://www.ing.iac.es/Astronomy/instruments/acam/

[4] The acronym IDL stands for Interactive Data Language and is a trademark of ITT Visual Information Solutions. For further details see http://www.ittvis.com/ProductServices/IDL.aspx.

[5] The ASTROLIB subroutine library is distributed by NASA. For further details see http://idlastro.gsfc.nasa.gov/.
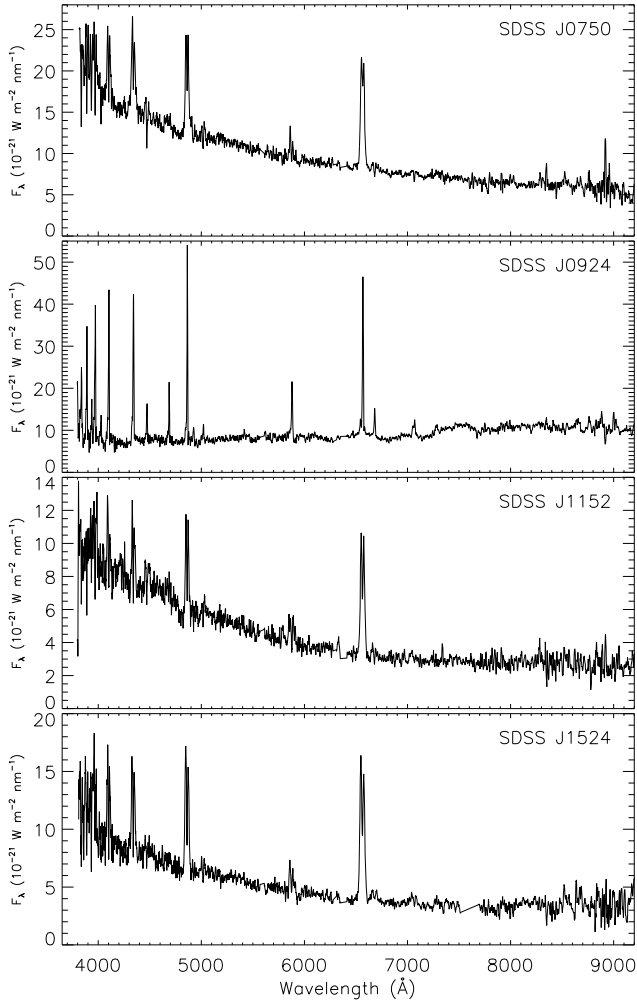
Fig. 1. SDSS spectra of the CVs for which we present orbital period measurements. For this plot the flux levels have been smoothed with 10-pixel Savitsky-Golay filters. The units of the abscissae are 10^{-21} W m^{-2} nm^{-1}, which corresponds to 10^{-17} erg s^{-1} cm^{-2} Å^{-1}.
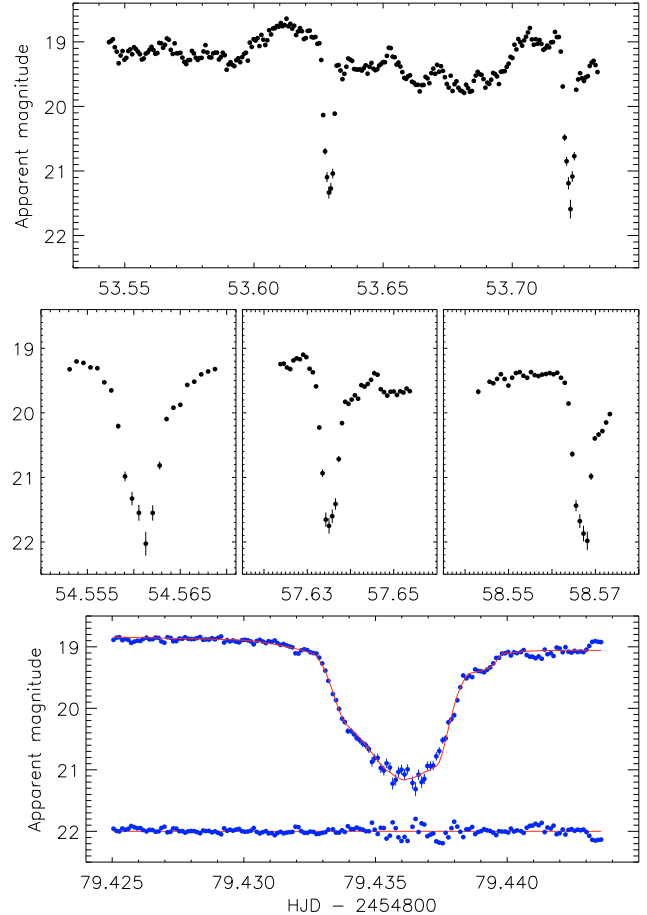

Fig. 2. Light curves of SDSS J0750. NTT data ($B_{\rm Tyson}$ filter) are shown on all panels except the bottom one, which contains the WHT data (V filter). The solid line represents our best LCURVE fit to the WHT data, and the residuals of the fit are plotted offset from zero for clarity. Note that the time axis has been stretched to suit each panel.

energy distribution of CVs, and the $B_{\rm Tyson}$ filter used at the NTT, the resulting apparent magnitudes are uncertain by at least a few tenths of a magnitude.

3. Light curve modelling

We have modelled the observed eclipses of SDSS J0750, SDSS J1152 and SDSS J1524 in order to explore the physical properties of these systems. For this analysis we used LCURVE, a code developed to fit light curves of eclipsing binary stars containing a degenerate object. A complete description of LCURVE is given in Copperwheat et al. (2010). The binary is defined by four components: white dwarf, secondary star, accretion disc and bright spot. We obtained initial fits using the Nelder-Mead downhill simplex and Levenberg-Marquardt methods (Press et al. 1992). We then used a Markov Chain Monte Carlo (MCMC) algorithm for final minimisation and determination of uncertainties (see Copperwheat et al. 2010).

We list the parameter determinations from these fits in Table 3. We include the following quantities: mass ratio (q), orbital inclination (i), time of white dwarf mid-eclipse (T_0), and the white dwarf radius and bright spot position expressed as fractions of the orbital semi-major axis ($r_{\rm WD}$ and $r_{\rm BS}$). We use the bright spot position as an indicator of the accretion disc radius,

since we assume that the bright spot lies at the outer edge of the accretion disc.

LCURVE implements a wealth of additional parameters which are needed for modelling high-precision data. The discovery data presented in this work are insufficient to constrain these parameters, so we fixed them at values which we have found to be physically appropriate in detailed modelling of other eclipsing systems (Copperwheat et al. 2010; Pyrzas et al. 2009; Nebot Gómez-Morán et al. 2009; Southworth et al. 2009a). Our fits are therefore only indicative, and definitive results will require high-quality follow-up light curves. We discuss the results for each system below.

4. SDSS J075059.97+141150.1

SDSS J0750 was identified by Szkody et al. (2007) as a CV from its SDSS spectrum, which shows a blue continuum with broad and double-peaked hydrogen Balmer and He I emission lines (Fig. 1). To our knowledge no other information is available in the literature for this object beyond a few catalogued magnitude measurements.

We observed SDSS J0750 on the night of 2009/01/20 using NTT/EFOSC2, detecting two eclipses in 4.5 h of observing (Fig. 2). It was in fact undergoing an eclipse whilst we tried to acquire it, although this was not clear at the time. We observed

Table 3. Parameter determinations from our LCURVE fits for SDSS J0750, SDSS J1152 and SDSS J1524.

Parameter			SDSS J0750	SDSS J1152	SDSS J1524
q	Mass ratio		0.59 ± 0.17	0.14 ± 0.03	0.17 ± 0.03
i	Orbital inclination	(°)	74.6 ± 1.9	83.7 ± 1.8	82.8 ± 0.8
T_0	Eclipse midpoint	(HJD)	$2454853.62917 \pm 0.00004$	$2454879.53815 \pm 0.00001$	$2454957.64961 \pm 0.00003$
r_{WD}	Radius of the WD	(a)	0.020 ± 0.004	0.012 ± 0.002	0.034 ± 0.002
r_{BS}	Bright spot position	(a)	0.16 ± 0.08	0.31 ± 0.04	0.29 ± 0.02

Notes. The radius of the WD and the radial position of the bright spot are given as fractions of a, the orbital semimajor axis.

Table 4. Measured times of eclipse for the objects studied in this work.

Object	Cycle	Time of eclipse (HJD)	Residual
SDSS J0750	0.0	$2\,454\,853.6293 \pm 0.0002$	-0.00003
SDSS J0750	1.0	$2\,454\,853.7225 \pm 0.0002$	-0.00001
SDSS J0750	10.0	$2\,454\,854.5612 \pm 0.0003$	0.00023
SDSS J0750	43.0	$2\,454\,857.6353 \pm 0.0002$	-0.00009
SDSS J0750	53.0	$2\,454\,858.5670 \pm 0.0003$	-0.00003
SDSS J0750	277.0	$2\,454\,879.4358 \pm 0.0001$	0.00000
SDSS J0924	0.0	$2\,454\,856.7192 \pm 0.0002$	-0.00013
SDSS J0924	1.0	$2\,454\,856.8104 \pm 0.0003$	-0.00007
SDSS J0924	11.0	$2\,454\,857.7220 \pm 0.0002$	0.00011
SDSS J0924	22.0	$2\,454\,858.7245 \pm 0.0002$	0.00006
SDSS J0924	250.0	$2\,454\,879.5046 \pm 0.0002$	-0.00001
SDSS J1152	0.0	$2\,454\,879.5388 \pm 0.0002$	
SDSS J1152	1.0	$2\,454\,879.6065 \pm 0.0002$	
SDSS J1524	0.0	$2\,454\,957.6499 \pm 0.0001$	
SDSS J1524	1.0	$2\,454\,957.7149 \pm 0.0003$	

Notes. These timings below were measured using the simple mirror-image method (Sect. 4) in order to maximise their archival value.

it again on subsequent nights during the same run, and with the WHT/ACAM a month later, in order to extend the time interval on which our orbital period measurement is based.

For each eclipse, a mirror-image of the light curve was shifted until the respective ascending and descending branches were in the best agreement. The time defining the axis of reflection was taken as the midpoint of the eclipses, and uncertainties were estimated based on how far this could be shifted before the agreement was visually poorer. We have fitted a linear ephemeris to these times of minimum light, finding

$$\mathrm{Min\,I\,(HJD)} = 2\,454\,853.62932(11) + 0.09316415(54) \times E$$

where E is the cycle number and the parenthesised quantities indicate the uncertainty in the last digit of the preceding number. This corresponds to an orbital period of 134.1564 ± 0.0008 min. The measured times of minimum light and the observed minus calculated values are given in Table 4.

4.1. Photometric model for SDSS J0750

We have modelled the WHT/ACAM light curve, which has the highest observing cadence, using the LCURVE code (Sect. 3). The best fit is shown in Fig. 2 and the parameters of the fit are given in Table 3. The relatively featureless light variation makes this quite a difficult object, and our mass ratio measurement is correspondingly uncertain (Table 3).

The photometric determination of parameters in CVs is dependent on measurement of the phase widths of the eclipses of the white dwarf and bright spot. The phase width of the white dwarf eclipse is intrinsically linked to i and q, causing these two

parameters to be degenerate (Bailey 1979). This degeneracy can be broken using the observed ingress and egress phases of the bright spot, but in the SDSS J0750 light curve these features are rather weakly defined. This causes a large uncertainty in the position of the bright spot and thus the mass ratio. High-speed photometry of several eclipses should be sufficient to provide a clear detection of the bright spot ingress and egress, and thus obtain a precise mass ratio (e.g. Littlefair et al. 2006, 2008; Copperwheat et al. 2010).

5. SDSS J092444.48+080150.9

SDSS J0924 is another new discovery from the SDSS survey, identified by Szkody et al. (2005) due to a spectrum which shows strong and narrow Balmer emission and hints of the secondary star towards the red end. The presence of strong He II is indicative of a magnetic system, but polarimetric observations revealed no polarisation. Szkody et al. (2005) presented follow-up observations comprising 11 spectra, which indicated an orbital period in the region of 2.1 h, and 3.75 h of photometry which showed clear variability but no eclipses.

We observed SDSS J0924 on the night of 2009/01/24 using the NTT, obtaining a light curve covering 3.75 h. These data cover two eclipses, which are approximately 2.5 mag deep and 10 min long (Fig. 3). We observed one additional eclipse on each of the two following nights, plus one more on the night of 2009/02/16 with the WHT. The eclipse midpoints were obtained as above and a straight line fitted to them to determine an ephemeris:

$$\mathrm{Min\,I\,(HJD)} = 2\,454\,856.71933(11) + 0.09114110(94) \times E$$

which equates to an orbital period of 131.2432 ± 0.0014 min. The measured times of minimum light and the observed minus calculated values are given in Table 4.

The ascending and descending branches of the eclipses of SDSS J0924 are extremely quick and are not resolved by our data, even though the WHT observations have a mean cadence of 15.2 s. The dominant light source in the system is therefore very small, which requires it to be all or part of the white dwarf. The Balmer emission lines indicate that there is mass transfer occuring in this system, but the eclipse morphology indicates that any accretion disc is rather faint. This is clear evidence that the white dwarf is magnetic and its field is disrupting the disc. This system is very well suited to the measurement of the radius of the white dwarf, although this would need high-speed photometry obtained using a large telescope. We did not attempt to model the light curve; our data do not resolve the eclipse ingress and egress shapes so the LCURVE solutions would be indeterminate.

It is not clear why eclipses were not detected by Szkody et al. (2005), although it must be remembered that the telescope available to these authors was much smaller (1.0 m versus 3.6 m).
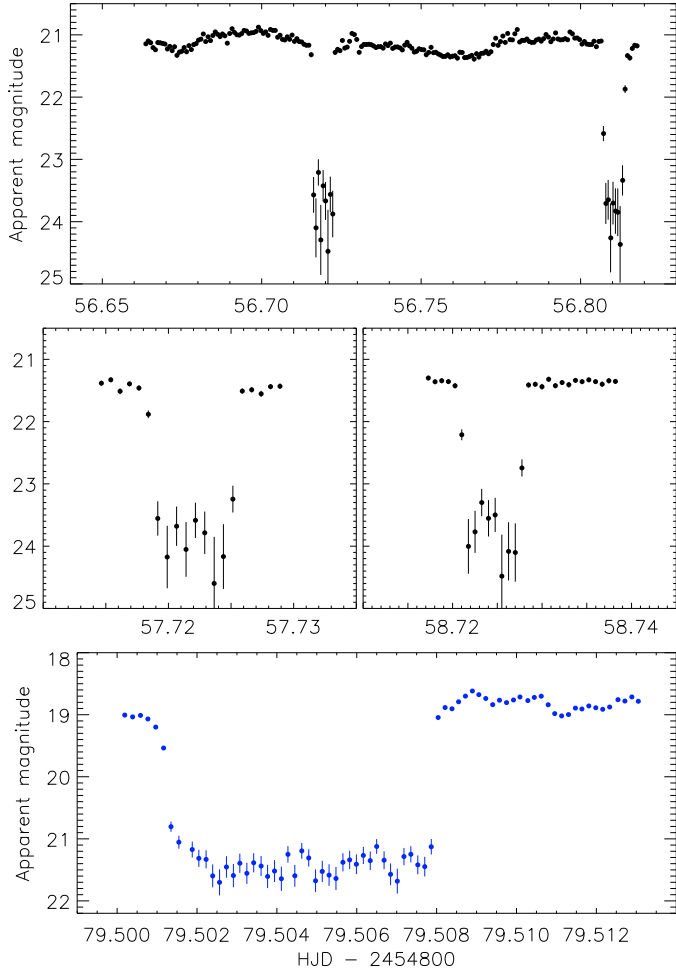
Fig. 3. Light curves of SDSS J0924. NTT data (B_{Tyson} filter) are shown on all panels except the bottom one, which contains the WHT data (V filter). The time axis has been stretched to suit each panel.

Dr. A. Henden (private communication) has kindly supplied the data from Szkody et al. for a closer inspection. We find that their light curve closely matches the morphology of our own data from the night of 2009/01/24, and that it is possible to align the two eclipses we observed on that night with two short gaps in Szkody et al.'s data. Their non-detection therefore can be attributed to either bad luck with the observing conditions or equipment, or to accidental rejection of data where SDSS J0924 was in eclipse and thus below the detection limit of individual images.

5.1. Spectral energy distribution of SDSS J0924

The secondary star dominates the optical spectrum of SDSS J0924 at longer wavelengths, exhibiting potassium and sodium absorption lines as well as strong TiO bandheads characteristic of mid-to-late M dwarfs. We have determined the star's spectral type using an M dwarf template library (Rebassa-Mansergas et al. 2007). These templates were scaled and subtracted from the SDSS spectrum of SDSS J0924, and the smoothest residual spectrum was obtained for a spectral type of M2±0.5 (Fig. 4). Two SDSS spectra are available for this object, and they give consistent results. From this best-fitting template, we calculated f_{TiO}, the flux difference between the bands 7450–7550 Å and 7140–7190 Å (Beuermann 2006). For the orbital period of SDSS J0924, and an assumed mass ratio of $q = 0.25$,
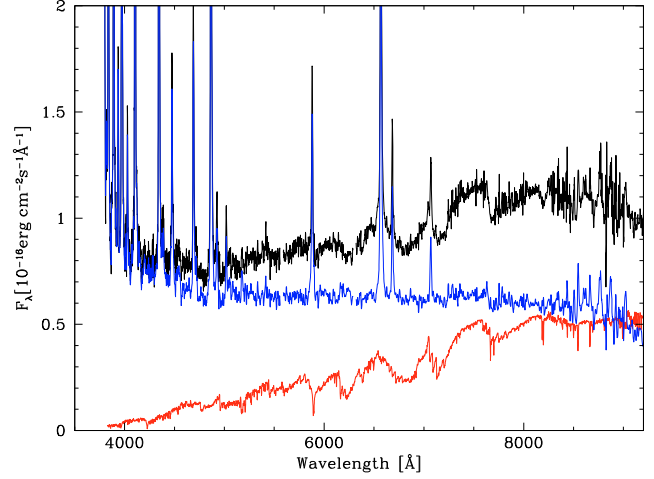

Fig. 4. Black line: the SDSS spectrum of SDSS J0924. Red line: an M2 template spectrum scaled to match the strengths of the spectral features of the secondary star. Blue line: the residual spectrum obtained after subtracting the M-dwarf template from the spectrum of SDSS J0924.
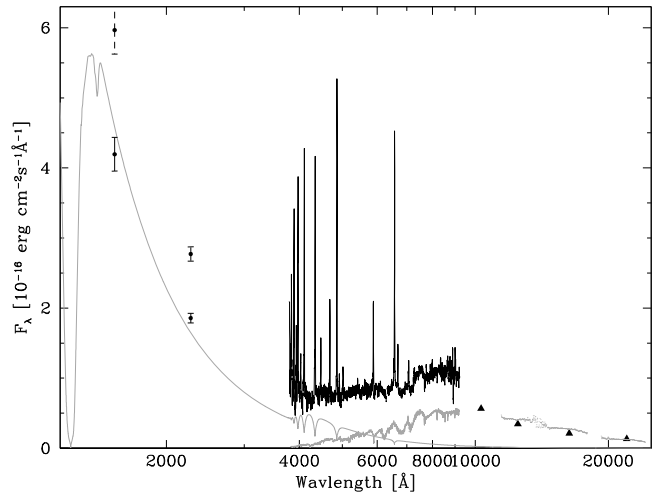

Fig. 5. Black line: the SDSS spectrum of SDSS J0924. Black dots: ultraviolet fluxes of SDSS J0924 from the GALEX Medium Imaging Survey (lower pair) and dereddened by the full galactic dust column (Schlegel et al. 1998), $E_{B-V} = 0.047$ (upper pair). Black triangles: UKIDSS $yJHK$ fluxes. Gray lines: best-fitting M2 secondary star spectrum from Fig. 4 and a white dwarf with $T_{\mathrm{eff}} = 17\,000$ K and $\log g = 8.3$, scaled for $d = 650$ pc, as a plausible match to the observed ultraviolet fluxes.

we find $R_2 = 0.23\,M_\odot$ (only weakly dependent on q). Using the polynomial expressions of Beuermann (2006), we find a distance of $d = 650 \pm 30$ pc.

SDSS J0924 has also been detected in the ultraviolet (UV) Medium Imaging Survey by GALEX (Morrissey et al. 2007) and in the infrared (IR) by UKIDSS (Lawrence et al. 2007). The UV-optical-IR spectral energy distribution is shown in Fig. 5. For a distance of 650 pc, the UV fluxes are consistent with a 15 000–20 000 K white dwarf, depending on its surface gravity (and hence mass). This temperature range is entirely consistent with that observed in a number of magnetic CVs (Townsley & Gänsicke 2009). Assuming a canonical mass for a CV white dwarf, $M_{\mathrm{wd}} = 0.8\,M_\odot$ and an effective temperature of 17 000 K, we find a good match to the GALEX fluxes and the blue upturn of the SDSS spectrum (Fig. 5).
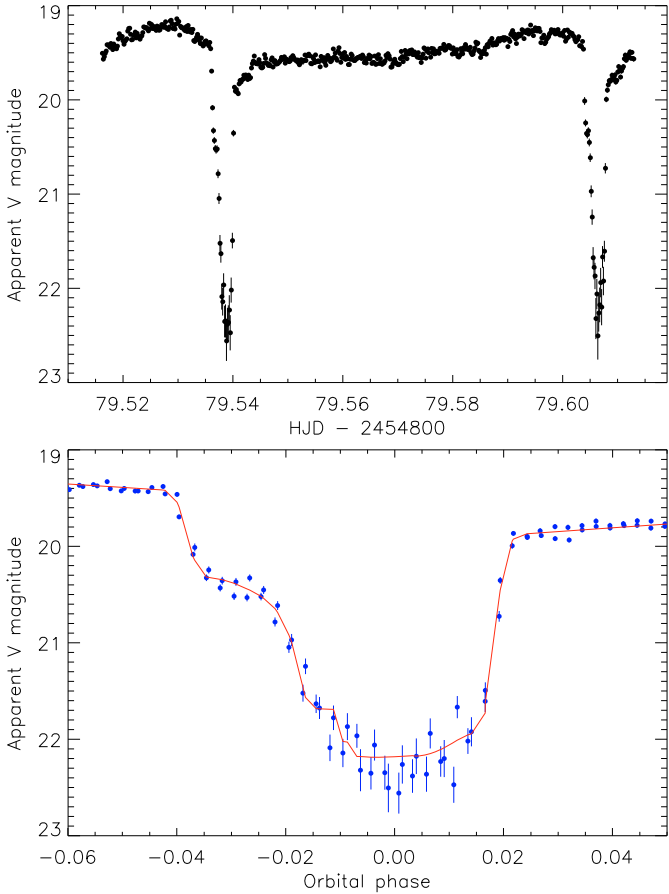
Fig. 6. The WHT light curve of SDSS J1152 against time (*upper panel*) and orbital phase (*lower panel*). The best fit is plotted with a solid line in the lower panel.

For a system at the lower edge of the period gap, Beuermann et al. (1998) and Knigge (2006) suggest that the companion should be an M4 dwarf. The spectral type of the companion star determined from the SDSS spectrum, M2, is hence too early for the orbital period of the system. This suggests that the donor star is somewhat evolved, similar to the dwarf nova QZ Ser, a $P_{\rm orb}$ = 119.8 min CV which harbours a K4 ± 2 companion star (Thorstensen et al. 2002). Ultraviolet spectroscopy of SDSS J0924 would allow us to probe the abundance ratio of nitrogen to carbon, which is expected to be enhanced in such stars by nuclear processing (Gänsicke et al. 2003)

6. SDSS J115207.00+404947.8

The SDSS spectrum of SDSS J1152 shows a blue continuum with broad double-peaked Balmer emission features, leading Szkody et al. (2007) to identify it as one of the population of SDSS CVs. The large separation of the double peaks is a telltale signature of a high orbital inclination, whilst the shallow Balmer absorption outside the emission lines is a clear sign of the underlying white dwarf.

The spectral features of SDSS J1152 are a reliable indicator of a high-inclination short-period CV with a low mass transfer rate (e.g. SDSS J1035; Southworth et al. 2006; and Littlefair et al. 2006), and our observations indeed reveal two deep eclipses recurring on a period close to the minimum found in hydrogen-rich CVs (Fig. 6). Due to poor weather we were unable to obtain additional data, so the ephemeris is not precise:

Min I (HJD) = 2 454 879.5388(2) + 0.06770(28) × E
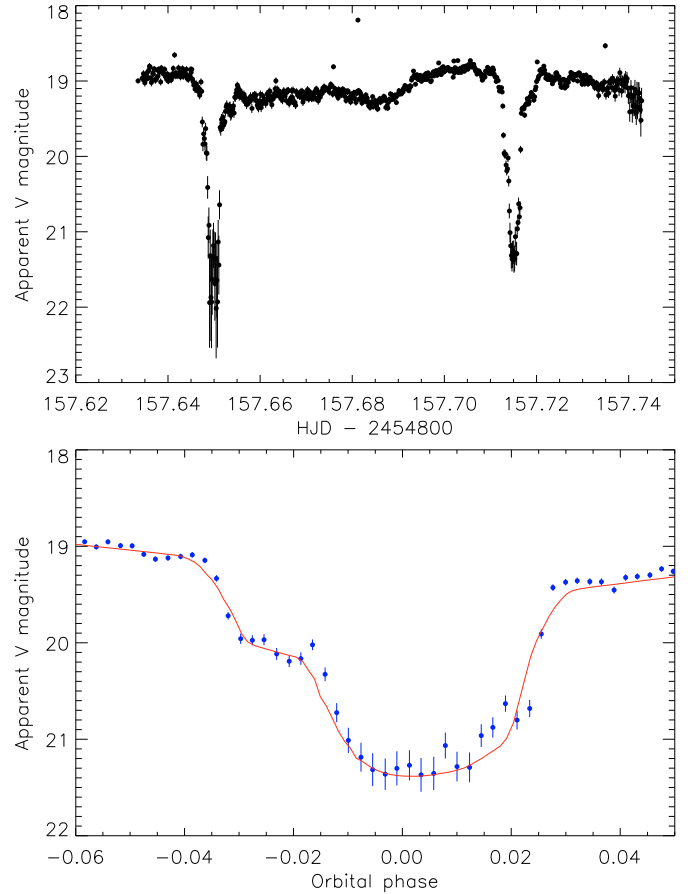corresponding to an orbital period of 97.5 ± 0.4 min.

Fig. 7. Our WHT light curve of SDSS J1524 against time (*upper panel*) and orbital phase (*lower panel*). Only the second eclipse is plotted in the lower panel, as these data are much better than those from the first eclipse. The best fit (solid line in the lower panel) is compromised by the slightly different shape of the first eclipse (not shown) compared to the second eclipse.

The phased light curve in Fig. 6 clearly shows that the bright spot and the white dwarf are eclipsed. This makes SDSS J1152 a good candidate for measurement of its physical properties: we have modelled our data using LCURVE (Sect. 3) and find that the mass ratio is well-defined even though our observations are rather noisy. High-quality follow-up observations of SDSS J1152 are strongly encouraged.

7. SDSS J152419.33+220920.1

SDSS J1524 was discovered to be a CV by Szkody et al. (2009), from an SDSS spectrum which is very similar to that of SDSS J1152. Szkody et al. stated that the deep central absorption in the centres of the double-peaked Balmer emission made it a candidate eclipsing system. Our follow-up photometry, obtained over 2.75 h on the night of 2009/05/06 using the WHT in service mode, confirms this suggestion. We observed two eclipses, which have a depth of 2.2 mag and a duration of 5.6 min and show clear structure due to the eclipse of the bright spot and of the white dwarf (Fig. 7). We find an ephemeris of

Min I (HJD) = 2 454 957.6499(1) + 0.06500(32) × E

corresponding to an orbital period of 93.6 ± 0.5 min. The measured times of minimum light are given in Table 4.

SDSS J1524 is strongly reminiscent of SDSS J1152, and our LCURVE models of the two systems are very similar (Table 3). Our modelling of the eclipses of SDSS J1524 was hindered by flickering, which causes the two eclipses to have different shapes. SDSS J1524 is, however, an excellent candidate for detailed characterisation using high-speed photometry, as flickering can be averaged out by observing several eclipses.

Since our observations were taken we have become aware that Dr. J. Patterson has independently discovered eclipses in SDSS J1524[6]. An outburst has also been detected by the *Catalina Sky Survey* (CSS Drake et al. 2009) using a 0.7 m Schmidt telescope, which allows us to classify this system as a dwarf nova.

8. Five SDSS cataclysmic variables showing no periodic brightness variations

During our NTT observing run we obtained light curves of five CVs which did not display any clear periodic variability. Their spectra are shown in Fig. 8, the log of observations is given in Table 2, and our light curves are plotted in Fig. 9. Orbital period measurements of these objects will require spectroscopic observations, mostly with a large telescope.

We obtained a single 2.75 h light curve of SDSS J0310 (Szkody et al. 2003): there is a hint of a brightness variation at 76 min but it is not significant enough to claim a detection. SDSS J0310 appears to outburst quite frequently. It was at magnitude $g = 15.5$ in the SDSS imaging observations, but at $g_{spec} = 22.0$ in the subsequent SDSS spectroscopic observations. Szkody et al. then found it to be in outburst during their follow-up spectroscopic observations. An outburst was also observed by Berto Monard[7], where superhumps were visible with a period of either 0.0643(3) d or its one-day alias of 0.0687(3) d[8].

We observed SDSS J0743 (Szkody et al. 2006) on the night of 2009/01/23, for 2 h then another 1 h after a gap of 2 h. The light curve shows nothing out of the ordinary. One outburst has been seen for this CV in 2006 October, by the CSS (Drake et al. 2009), where it increased in brightness by at least 5 mag.

SDSS J0746 was found to be a CV by Szkody et al. (2006) and is another object which was much brighter when the SDSS observed it photometrically ($g = 18.2$) than spectroscopically ($g_{spec} = 21.2$). The CSS has detected two outbursts in which the object became as bright as magnitude 16 (Drake et al. 2009). Nakajima[9,10] and Maehara[11] have reported a measurement of the superhump period of 0.06666(3) d. Our own light curve covers a total of 3.75 h over two observing sequences on the night of 2009/01/23 (Fig. 9). We confirm that SDSS J0746 is a very variable object, but in this case we find only stochastic variations with a total amplitude of 1.3 mag and attributable to the phenomenon of flickering (Bruch 1992, 2000).

We observed SDSS J0758 (Szkody et al. 2009) for only 2.3 h in two segments on the night of 2009/01/25. The light curve shows some variation but our data are insufficient to be useful for period measurement. We have a short sequence of spectroscopic observations from 2008 February which indicate a period of about 80 min and will be presented in a later paper.
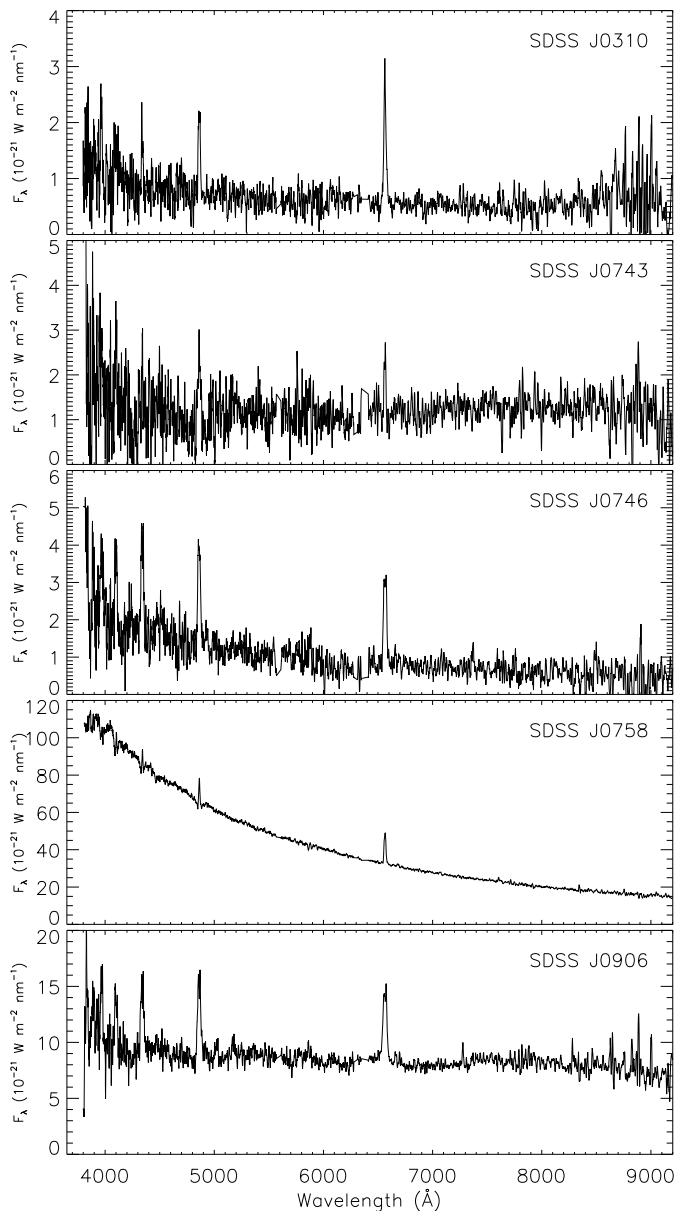
---

[6] See http://cbastro.org/
[7] vsnet-alert number 8239
[8] vsnet-gcvs number 614
[9] vsnet-alert number 11069
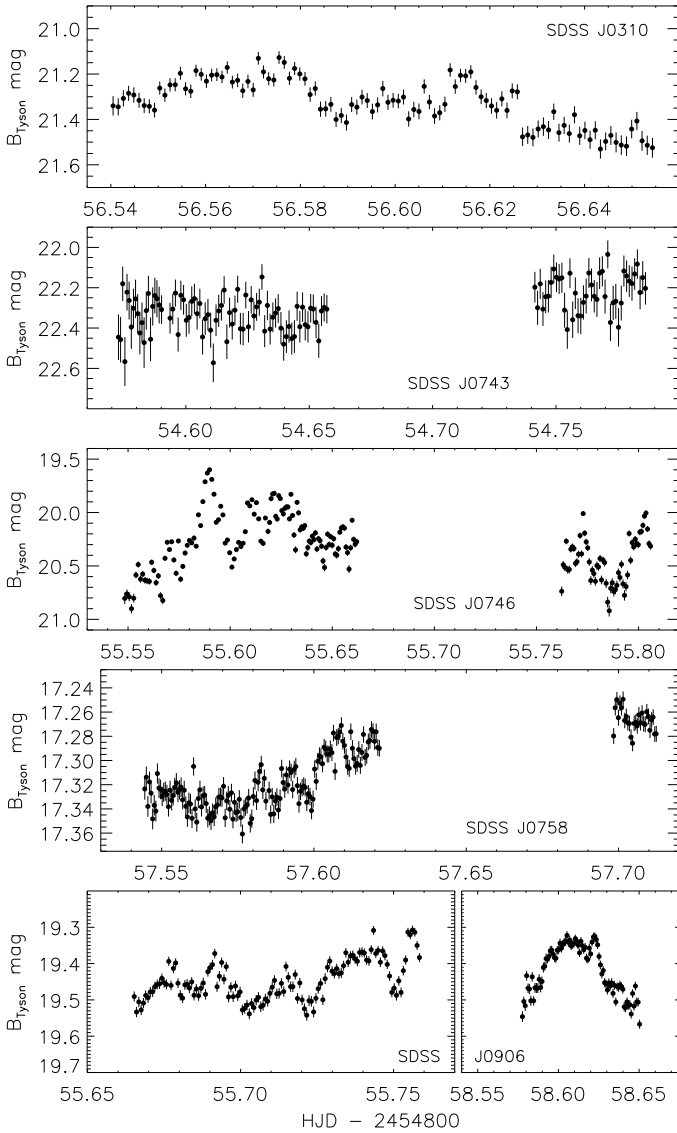[10] vsnet-outburst number 10022
[11] vsnet-alert number 11075

Fig. 8. SDSS spectra of the CVs for which we did not find periodic brightness variations. See Fig. 1 caption for details.

SDSS J0906 was found to be a CV by Szkody et al. (2005) from an SDSS spectrum which shows moderately weak Balmer line emission. Twelve outbursts, of amplitude roughly 3 mag, have been seen by the CSS (Drake et al. 2009), which makes it a frequently-outbursting system. Our 5.75 h of NTT observations, in three blocks over two nights, show 0.2 mag brightness variations but nothing which is clearly periodic. We have also obtained 4.8 h of INT photometry of this system (Fig. 10) which shows similar characteristics.

9. Summary and discussion

We have presented NTT/EFOSC2 and WHT/ACAM time-series photometry of nine CVs identified by the SDSS, from which we find four of them to be eclipsing systems. We also present light curves of five SDSS CVs which do not show identifiable periodic phenomena. Our results are summarised in Table 5.

Fig. 9. NTT light curves of SDSS J0310, SDSS J0743, SDSS J0746, SDSS J0758 and SDSS J0906.

Fig. 10. The INT light curves of SDSS J0906.

Table 5. Summary of the orbital periods and CV classification obtained for the objects studied in this work.

Object	Period (min)	Notes
SDSS J0310		Dwarf nova, unknown period
SDSS J0743		Dwarf nova, unknown period
SDSS J0746		Dwarf nova, unknown period
SDSS J0750	134.1564 ± 0.0008	Eclipsing CV
SDSS J0758		CV, no observed periodicity
SDSS J0906		Dwarf nova, unknown period
SDSS J0924	131.2432 ± 0.0014	Eclipsing magnetic CV
SDSS J1152	97.5 ± 0.4	Eclipsing CV
SDSS J1524	93.6 ± 0.5	Eclipsing dwarf nova

SDSS J0750 has an orbital period of 134.1564 min, which puts it in an interesting situation close to the lower edge of the 2–3 h period gap in the observed population of CVs (Whyte & Eggleton 1980; Knigge 2006). This period gap is commonly explained through the phenomenon of disrupted magnetic braking (Spruit & Ritter 1983), which requires CVs to migrate through the gap without undergoing mass transfer. A prediction of this scenario is that CVs with orbital periods of 2 h have secondary star masses essentially the same as those with periods of 3 h; SDSS J0750 fits the bill perfectly as a 2 h CV whose donor mass can be measured precisely.

SDSS J0924 has an orbital period of 131.2432 min. It displays strong He II emission and has an extremely faint or missing accretion disc, so is very likely to be a magnetic CV. As magnetic CVs evolve differently from their non-magnetic cousins (Webbink & Wickramasinghe 2002), SDSS J0924 is precluded from investigations of the disrupted magnetic braking scenario. Instead, the shape of the eclipse suggests that it will be possible to measure the radius of the WD directly. Our own observations have a cadence of 15 s and do not resolve the ingress and egress o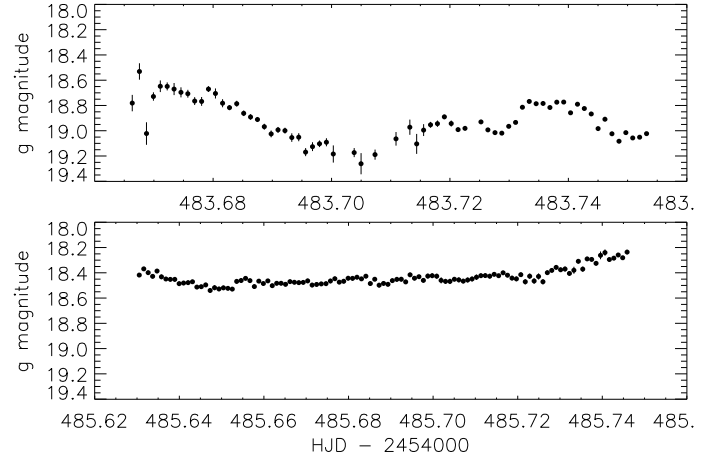f the WD. Light curves with a substantially higher time resolution, such as can be provided by ULTRACAM (Dhillon et al. 2007), will be necessary.

SDSS J1152 and SDSS J1524 are near-identical twins, for which we find orbital periods of 97.5 and 93.6 min and mass ratios of 0.14 and 0.17, respectively. Ingress and egress features of both the WD and the bright spot are clearly visible in our light curves, which makes these objects very well suited to photometric determinations of their physical properties (e.g. Littlefair et al. 2007, 2008).

Five of our nine targets did not exhibit identifiable periodic brightness variations; of these SDSS J0746 shows a remarkable flickering activity with an amplitude of at least 1.3 mag. Time-resolved spectroscopy is needed to measure the orbital periods of these objects, which will require 8m-class telescopes.

All four of the orbital periods measured in this work are shorter than the 2–3 h period gap observed in the general CV population. This is an increasingly common feature of the SDSS sample of CVs, and further evidence that previous samples are much less complete for the shorter-period faint systems than for the longer-period and generally much brighter objects (Gänsicke et al. 2009). The SDSS CV sample is a unique window into the physical properties and evolutionary history of this faint but dominant population of CVs.

Data System; the SIMBAD database operated at CDS, Strasbourg, France; and the arχiv scientific paper preprint service operated by Cornell University.

References

Bailey, J. 1979, MNRAS, 187, 645
Bertin, E., & Arnouts, S. 1996, A&AS, 117, 393
Beuermann, K. 2006, A&A, 460, 783
Beuermann, K., Baraffe, I., Kolb, U., & Weichhold, M. 1998, A&A, 339, 518
Bruch, A. 1992, A&A, 266, 237
Bruch, A. 2000, A&A, 359, 998
Buzzoni, B., Delabre, B., Dekker, H., et al. 1984, The Messenger, 38, 9
Copperwheat, C. M., Marsh, T. R., Dhillon, V. S., et al. 2010, MNRAS, 402, 1824
de Kool, M. 1992, A&A, 261, 188
de Kool, M., & Ritter, H. 1993, A&A, 267, 397
Dhillon, V. S., Marsh, T. R., Stevenson, M. J., et al. 2007, MNRAS, 378, 825
Dillon, M., Gänsicke, B. T., Aungwerojwit, A., et al. 2008, MNRAS, 386, 1568
Downes, R. A., Webbink, R. F., Shara, M. M., et al. 2001, PASP, 113, 764
Drake, A. J., Djorgovski, S. G., Mahabal, A., et al. 2009, ApJ, 696, 870
Gänsicke, B. T., Szkody, P., de Martino, D., et al. 2003, ApJ, 594, 443
Gänsicke, B. T., Araujo-Betancor, S., Hagen, H.-J., et al. 2004, A&A, 418, 265
Gänsicke, B. T., Rodríguez-Gil, P., Marsh, T. R., et al. 2006, MNRAS, 365, 969
Gänsicke, B. T., Dillon, M., Southworth, J., et al. 2009, MNRAS, 397, 2170
Hellier, C. 2001, Cataclysmic Variable Stars: How and Why they Vary, Springer-Praxis books in astronomy and space science (New York: Springer Verlag)
Jordi, K., Grebel, E. K., & Ammon, K. 2006, A&A, 460, 339
Knigge, C. 2006, MNRAS, 373, 484
Kolb, U. 1993, A&A, 271, 149
Kolb, U., & Baraffe, I. 1999, MNRAS, 309, 1034
Kolb, U., & de Kool, M. 1993, A&A, 279, L5
Lawrence, A., Warren, S. J., Almaini, O., et al. 2007, MNRAS, 379, 1599
Littlefair, S. P., Dhillon, V. S., Marsh, T. R., et al. 2006, Science, 314, 1578
Littlefair, S. P., Dhillon, V. S., Marsh, T. R., et al. 2007, MNRAS, 381, 827
Littlefair, S. P., Dhillon, V. S., Marsh, T. R., et al. 2008, MNRAS, 388, 1582
Morrissey, P., Conrow, T., Barlow, T. A., et al. 2007, ApJS, 173, 682
Nebot Gómez-Morán, A., Schwope, A. D., Schreiber, M. R., et al. 2009, A&A, 495, 561
Politano, M. 1996, ApJ, 465, 338
Politano, M. 2004, ApJ, 604, 817
Press, W. H., Teukolsky, S. A., Vetterling, W. T., & Flannery, B. P. 1992, Numerical recipes in FORTRAN 77. The art of scientific computing (2nd edn.) (Cambridge: University Press)
Pyrzas, S., Gänsicke, B. T., Marsh, T. R., et al. 2009, MNRAS, 394, 978
Rebassa-Mansergas, A., Gänsicke, B. T., Rodríguez-Gil, P., Schreiber, M. R., & Koester, D. 2007, MNRAS, 382, 1377
Ritter, H., & Kolb, U. 2003, A&A, 404, 301
Schlegel, D. J., Finkbeiner, D. P., & Davis, M. 1998, ApJ, 500, 525
Southworth, J., Gänsicke, B. T., Marsh, T. R., et al. 2006, MNRAS, 373, 687
Southworth, J., Gänsicke, B. T., Marsh, T. R., de Martino, D., & Aungwerojwit, A. 2007a, MNRAS, 378, 635
Southworth, J., Marsh, T. R., Gänsicke, B. T., et al. 2007b, MNRAS, 382, 1145
Southworth, J., Gänsicke, B. T., Marsh, T. R., et al. 2008a, MNRAS, 391, 591
Southworth, J., Townsley, D. M., & Gänsicke, B. T. 2008b, MNRAS, 388, 709
Southworth, J., Hickman, R. D. G., Marsh, T. R., et al. 2009a, A&A, 507, 929
Southworth, J., Hinse, T. C., Burgdorf, M. J., et al. 2009b, MNRAS, 399, 287
Southworth, J., Hinse, T. C., Dominik, M., et al. 2009c, ApJ, 707, 167
Southworth, J., Hinse, T. C., Jørgensen, U. G., et al. 2009d, MNRAS, 396, 1023
Spruit, H. C., & Ritter, H. 1983, A&A, 124, 267
Stetson, P. B. 1987, PASP, 99, 191
Szkody, P., Fraser, O., Silvestri, N., et al. 2003, AJ, 126, 1499
Szkody, P., Henden, A., Fraser, O. J., et al. 2005, AJ, 129, 2386
Szkody, P., Henden, A., Agüeros, M., et al. 2006, AJ, 131, 973
Szkody, P., Henden, A., Mannikko, L., et al. 2007, AJ, 134, 185
Szkody, P., Anderson, S. F., Hayden, M., et al. 2009, AJ, 137, 4011
Thorstensen, J. R., Fenton, W. H., Patterson, J., et al. 2002, PASP, 114, 1117
Townsley, D. M., & Gänsicke, B. T. 2009, ApJ, 693, 1007
Warner, B. 1995, Cataclysmic Variable Stars, Cambridge Astrophysics Series (Cambridge, UK: Cambridge University Press)
Webbink, R. F., & Wickramasinghe, D. T. 2002, MNRAS, 335, 1
Whyte, C. A., & Eggleton, P. P. 1980, MNRAS, 190, 801